

Effects of mean stress on the fatigue properties of core-in-sheath-type carbon/glass hybrid thermoplastic composite rods: Experimental investigation and practical predictive method

Hiroyuki Oguma¹  | Kimiyoshi Naito^{1,2} 

¹Research Center for Structural Materials, National Institute for Materials Science, Tsukuba, Japan

²Department of Aerospace Engineering, Tohoku University, Sendai, Japan

Correspondence

Hiroyuki Oguma, Research Center for Structural Materials, National Institute for Materials Science, Sengen 1-2-1, Tsukuba 305-0047, Ibaraki, Japan.

Email: oguma.hiroyuki@nims.go.jp

Funding information

Ministry of Education, Culture, Sports, Science and Technology; Japan Science and Technology Agency

Abstract

A systematic acquisition of fatigue test data was conducted under different stress ratio conditions to investigate the effect of mean stress on the fatigue properties of carbon/glass hybrid thermoplastic composite rods. Our findings revealed that as the stress ratio increased with a higher mean stress, the stress dependency of the fatigue life also increased, and the slope of the *S-N* curve became gentler. Under identical stress ratio conditions, hybrid rods with a greater volume fraction of carbon fiber exhibited the highest strength and a more gradual slope of the *S-N* curve. To account for mean stress effects, an equivalent stress amplitude was introduced, resulting in data collapse at around 10^7 cycles, rendering this approach an industrially useful method to predict fatigue behavior when working with limited experimental datasets. This study presents a practical technique for estimating fatigue strength under mean stress through a weighted average efficiency and equivalent stress amplitude.

KEYWORDS

carbon/glass hybrid, composite, fatigue properties, mean stress, strength estimation

Highlights

- This study empirically explores how mean stress influences carbon/glass hybrid rods.
- Our findings unveil the correlation between material structure and fatigue performance.
- A practical method for estimating fatigue strength, which considers mean stress, is proposed.

This is an open access article under the terms of the [Creative Commons Attribution-NonCommercial-NoDerivs](https://creativecommons.org/licenses/by-nc-nd/4.0/) License, which permits use and distribution in any medium, provided the original work is properly cited, the use is non-commercial and no modifications or adaptations are made.

© 2024 The Authors. *Fatigue & Fracture of Engineering Materials & Structures* published by John Wiley & Sons Ltd.

1 | INTRODUCTION

Over the past few years, the application of continuous fiber-reinforced polymers (FRPs) in various fields, including aerospace, automotive industry, and civil and architectural engineering, has been expanding due to their advantageous properties, such as high strength, light weight, corrosion resistance, and non-magnetic properties.¹ A very efficient way to maximize the advantages of FRPs is to apply them as a tensioned materials in ground anchors, prestressed concrete members, cable-stayed bridges, suspension bridges, and so on.^{2–6} Their specific fatigue life depends on their design, layup, and manufacturing process, as well as load conditions and environmental factors. Basic research on the mechanical properties of FRPs, including their application to various structures, is being actively conducted. Consequently, data on fatigue,^{7,8} creep, and relaxation⁹ are continuously gathered and evaluated to ensure their long-term safety and reliability.

Recently, novel core-in-sheath carbon/glass hybrid thermoplastic composite rods have been developed to take advantage of their excellent hybridization performance.¹⁰ The high strength-to-weight ratio, excellent stiffness, and high temperature resistance of carbon fibers are well known. In contrast, glass fibers offer good impact resistance, cost-effectiveness, and relatively easy handling during the manufacturing process. When these two types of fibers are combined in a hybrid material, their distinct properties complement each other, resulting in the development of a composite with balanced strength, stiffness, impact resistance, and cost efficiency.¹¹ Furthermore, this hybrid material can be tailored to achieve a desired balance between carbon and glass fibers characteristics, rendering it suitable for various industries where specific performance requirements need to be met. For example, hybrid thermoplastic composite rods have been introduced in Japan for use in the anti-seismic reinforcement of architectural structures.¹²

In previous studies, the physical and static properties of the carbon/glass hybrid thermoplastic composite rods have been investigated.^{13–16} In addition, the key factors influencing the fatigue properties of these hybrid rods were identified through a fatigue testing campaign.¹⁷ Based on the structure and degree of dispersion of hybrid rods, a simple parallel model was employed to predict fatigue behavior. The results suggest that a stress-based approach could accurately estimate the fatigue strength of hybrid rods. Although, cyclic loading conditions under various average stresses are conceivable,^{18–20} especially when considering

the actual use environment of these rods, the actual effect of mean stress on their fatigue properties has not yet been the subject of detailed analysis. Consequently, the present study conducted fatigue tests on carbon fiber/glass fiber hybrid rods under various stress ratios $R (= \sigma_{min}/\sigma_{max})$. The effects of mean stress on fatigue strength properties were investigated. Furthermore, we discuss various methods for predicting the criteria of failure, including the effect of mean stress using an equivalent stress amplitude.

2 | EXPERIMENTAL PROCEDURES

2.1 | Materials

The materials tested in this study were core-in-sheath carbon/glass hybrid thermoplastic rods as shown in Figure 1, namely, CABKOMA, developed by KOMATSU MATERE Co., Ltd.¹² Three types of hybrid rods with different carbon fiber contents and carbon/glass fiber ratios were used. Each rod was designated as 24K1P (one 24K tow), 24K2P, or 24K3P. Details of the physical and mechanical properties are given in the literature¹⁷ and in Appendix A.

2.2 | Testing conditions

Uni-axial fatigue tests were performed under sinusoidal loading using electro-servo hydraulic testing machines (SERVOPULSER EHF-E, Shimadzu Corporation and 858 Mini Biomix, MTS System Corporation). The gripping parts of the samples were fabricated using the wet hand layup process,^{21,22} and the gauge length of the fatigue specimen was 50 mm.¹⁷ The stress ratio, that is, the ratio of minimum stress to maximum stress in one cycle of loading cycle, $R = \sigma_{min}/\sigma_{max}$, was set as 0.1, 0.5, 0.7, or 0.9. The test frequency was 10 Hz, and the tests were terminated at 10^7 cycles. All tests were performed under laboratory conditions at room temperature ($RT = 23^\circ\text{C} \pm 3^\circ\text{C}$, $RH = 50\% \pm 5\%$). Fracture parts were observed using a scanning electron microscope (SEM) (Quanta 200, FEI).

3 | TEST RESULTS AND FRACTURE PART OBSERVATIONS

3.1 | Fatigue test results

The results of fatigue tests under various stress ratios are shown in Figure 2 as a double logarithmic plot. The

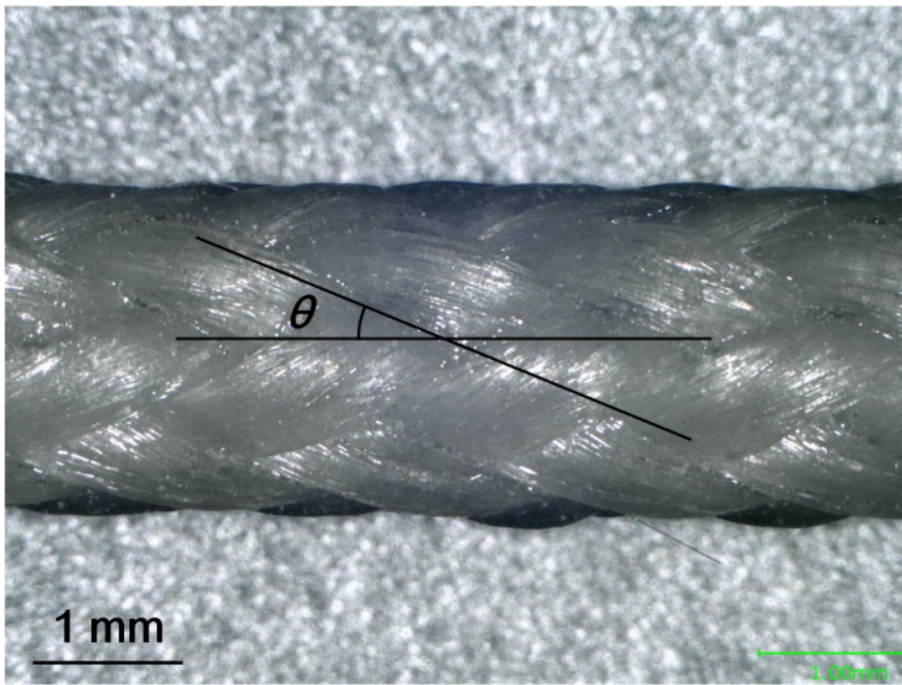


FIGURE 1 Appearance of a hybrid rod (θ : braid angle).¹⁷ [Colour figure can be viewed at wileyonlinelibrary.com]

vertical axis shows the maximum stress, σ_{max} , with the number of cycles to failure, N_f , on the horizontal axis. The regression lines in Figure 2 were obtained by the least squares method using the failed sample data as follows:

$$\sigma_{max} = a(N_f)^b \quad (1)$$

The coefficients obtained from this process are also summarized in Figure 2. Overall, the exponent b became larger (gentler slope of the $S-N$ curve) with increasing the stress ratio, suggesting that stress dependency of the fatigue life became larger under higher mean stress conditions. Typical of carbon fiber and CFRP (Carbon-fiber reinforced polymer) fatigue test results is the gentle slope observed in the $S-N$ curve.^{23–25} Under the same stress ratio conditions, 24K3P with higher volume fraction of carbon fiber had the greatest strength and the gentle slope of the $S-N$ curve, indicating that the carbon fiber core part dominates the fatigue properties of the hybrid rod. The difference in the stress dependency of the fatigue life was more clearly observed under $R = 0.1$, and the $S-N$ curve of 24K1P with higher volume fraction of void exhibited a steep slope. This, in turn, confirmed that voids in the hybrid rod had a greater effect under smaller σ_{min} in cyclic loading.

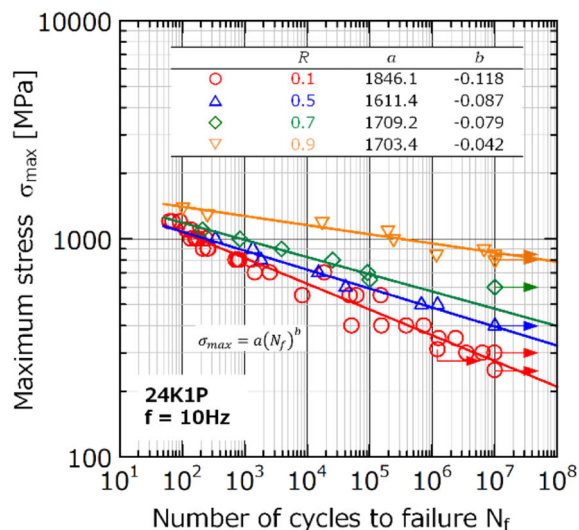
The fatigue strength at 10^7 cycles was obtained from the regression line according to Equation (1) and summarized in Figure 3. The stress amplitude σ_a and mean stress σ_{mean}

are represented on the vertical and horizontal axes, respectively. The fatigue strength in stress amplitude decreased with increasing mean stress. Several models have been proposed to estimate the effect of mean stress on fatigue strength.²⁶ In this study, the data plots can be approximated by a straight line, which connects the tensile strength, $\sigma_{L,ult}$ (24K1P: 1423 MPa, 24K2P: 1804 MPa, 24K3P: 1837 MPa),¹⁷ on the abscissa and the fatigue strength under $R = 0.1$; however, some of the data were plotted on the lower side of the line. This result indicates that the use of a linear relationship to estimate the effect of mean stress on fatigue strength may be on the dangerous side. Applying a downward convex curve was expected to more accurately explain the trend of the experimental data.

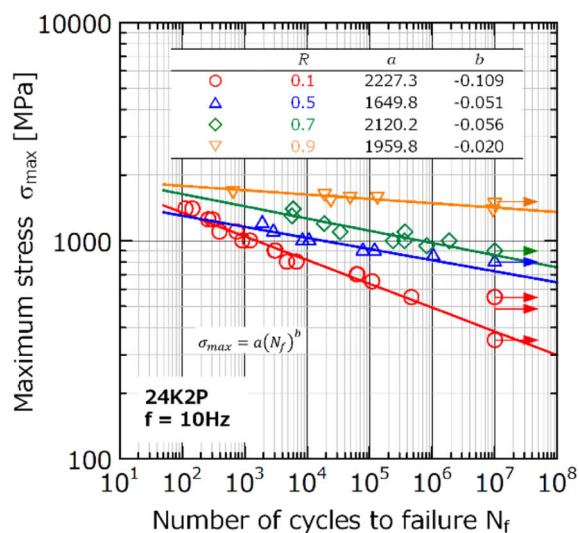
The equivalent stress amplitude, defined by Equation (2), was introduced to rearrange the fatigue test data with consideration of the mean stress correction.²⁷

$$\sigma_{eq} = \sqrt{\sigma_{max}\sigma_a} \quad (2)$$

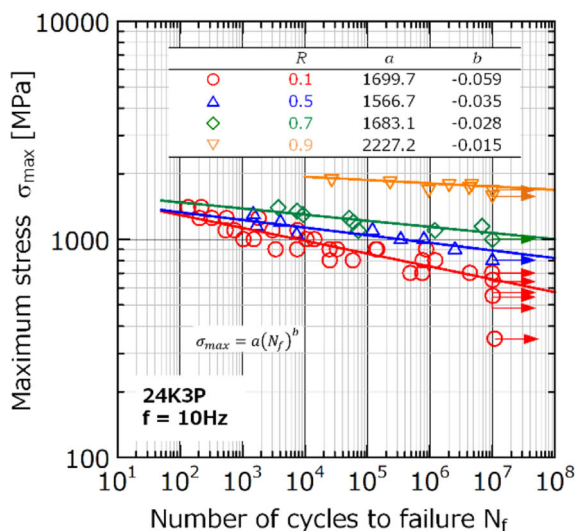
The rearranged data were subsequently organized in the log–log plot of the equivalent stress amplitude against fatigue life, as shown in Figure 4, and the regression lines were obtained with the least squares method. All data points with different stress ratios almost collapsed into a single line, particular at around 10^7 cycles. This result indicated that the fatigue strength in the long-life regime under different mean stress values could be estimated by using single fatigue data set obtained under a single stress ratio condition.



(A) 24K1P



(B) 24K2P



(C) 24K3P

FIGURE 2 Fatigue test results for (A) 24K1P, (B) 24K2P, and (C) 24K3P; the arrow indicates cut-off data. [Colour figure can be viewed at wileyonlinelibrary.com]

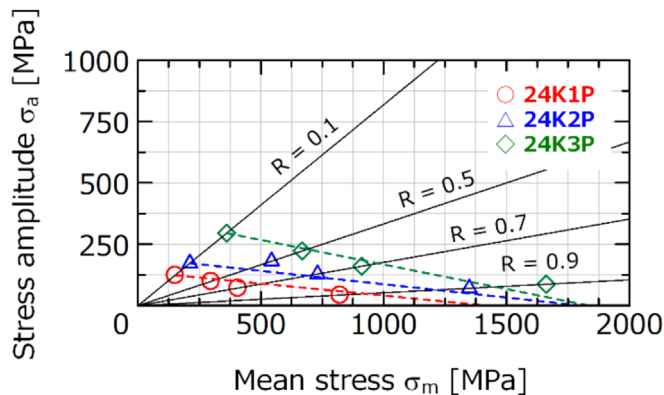
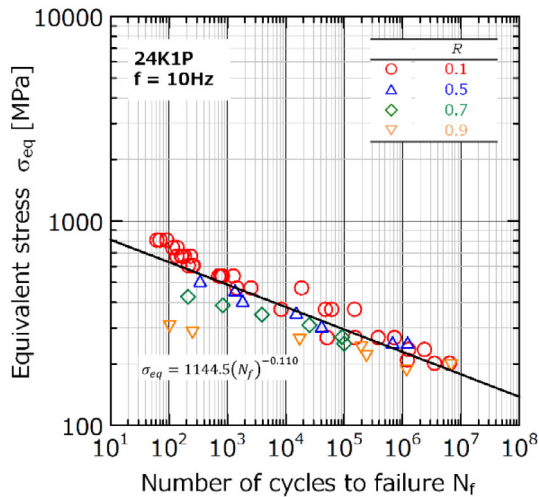


FIGURE 3 Constant life diagram for 10^7 loading cycles. [Colour figure can be viewed at wileyonlinelibrary.com]

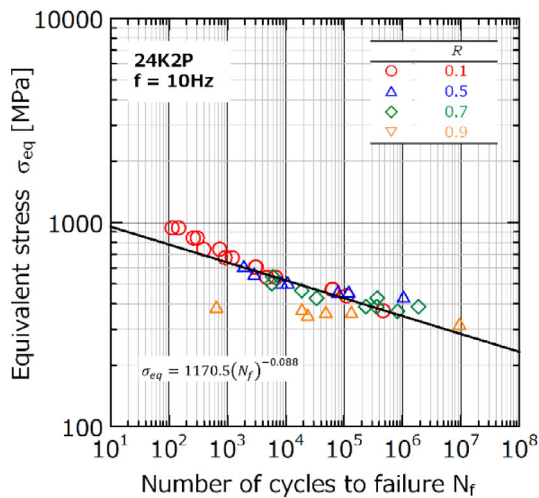
3.2 | Fracture part observations

Fatigue fracture occurred in the gauge part of the specimen, which were observed by SEM. The fractured parts of 24K1P are shown in Figure 5A–D. A rapid catastrophic fiber breakage phase occurred under higher stress conditions predominantly, and the matrix polymer clung to the carbon fiber, as shown in Figure 5A,B. In contrast, splitting of the carbon fiber bundles and pull-out of the carbon fibers were observed in the parts fractured at low-stress levels. In addition, carbon fiber fragments were frequently observed, as indicated by the arrows in Figure 5C. Under high stress ratio with high mean stress, pull-out and breakage of carbon fibers mainly occurred; however, fragments were not observed, as shown in Figure 5D. The fractured parts of 24K3P are shown in Figure 6. Also, polymers clinging to carbon fibers were more frequently observed. This tendency was probably due to a lower volume fraction of void¹⁷ and related to the higher fatigue strength and gentler slope of the S-N curve of 24K3P than that of 24K1P and 2P.

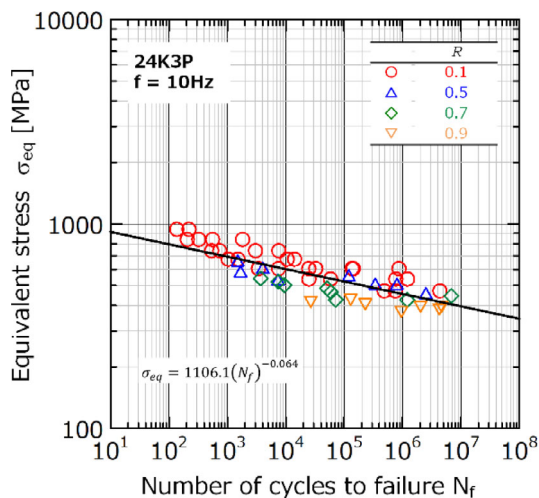
In a prior investigation, X-ray computed tomography demonstrated that elongated and needle-like voids were randomly dispersed throughout the bundles of carbon fibers.¹⁷ These voids had an impact on force transmission between the fibers and could potentially initiate a fatigue crack. Additionally, fiber waviness decreased the fatigue life. Bending or



(A) 24K1P



(B) 24K2P



(C) 24K3P

FIGURE 4 Relationship between equivalent stress amplitude and cycles to failure for (A) 24K1P, (B) 24K2P, and (C) 24K3P. [Colour figure can be viewed at wileyonlinelibrary.com]

buckling of carbon fibers under minimal cyclic stress in small stress ratio conditions might have resulted in localized failure. Under higher mean stress conditions, fibers were held in a tensioned state, and the effect of waviness became smaller, changing the load distribution and stress dependency of fatigue life.

4 | DISCUSSION

4.1 | Fatigue strength estimation using test data under one stress ratio condition

In Section 3.1, it was expected that the fatigue strength under different mean stress conditions could be estimated using only one fatigue test dataset, that is, one $S-N$ curve. The fatigue test data obtained under $R = 0.1$ were rearranged using the equivalent stress amplitude and summarized in Figure 7. The regression line expressed by Equation (3) was obtained with the least squares method, and the fatigue strength at 10^7 cycles was estimated by Equation (4), as shown in Figure 8. The lines obtained from this equation were found to be in good agreement with the test results, and therefore, the effect of mean stress on the fatigue strength was well expressed. This, in turn, indicates that the fatigue strength under different mean stress conditions can be estimated by using only one $S-N$ curve of the fatigue test, while the introduction of equivalent stress amplitude is an industrially useful method to predict fatigue behavior when working with limited experimental data sets.

$$\sigma_{eq} = \sqrt{\sigma_{max}\sigma_a} = \sqrt{(\sigma_a + \sigma_m)\sigma_a} = a(N_f)^b \quad (3)$$

$$\sqrt{(\sigma_a + \sigma_m)\sigma_a} = a(10^7)^b \quad (4)$$

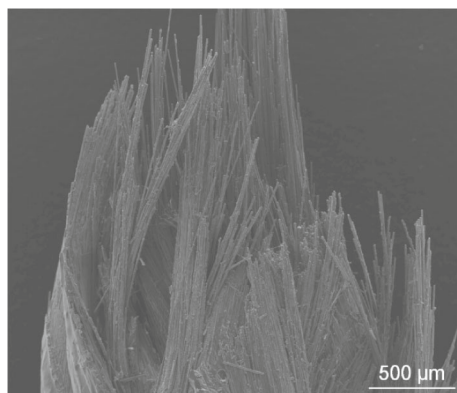
4.2 | Estimation of the fatigue strength using CFRP and GFRP test data

A previous study estimated the fatigue properties of a hybrid rod using test data of unidirectional CFRP and GFRP (Glass-fiber reinforced polymer) based on the volume fraction of fibers and the weighted average efficiency as follows¹⁷:

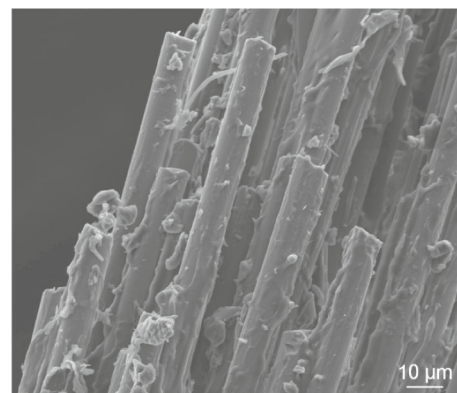
$$\sigma_{Hybrid} = \frac{VF_{CF}\sigma_{CF_CFRP} + \Phi VF_{GF}\sigma_{GF_GFRP}}{2} \quad (5)$$

where the coefficient $\Phi = \cos\theta$ was introduced to consider the effect of the braid angle in the hybrid rod. VF_{CF} and VF_{GF} represent the volume fraction of carbon fiber

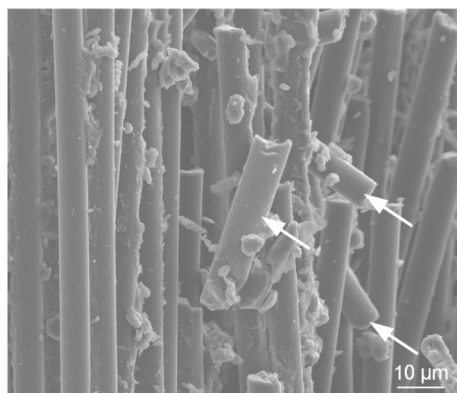
FIGURE 5 Images of 24K1P fracture parts fractured during the fatigue tests (R : stress ratio; σ_{max} : maximum stress; and N_f : number of cycles to failure).



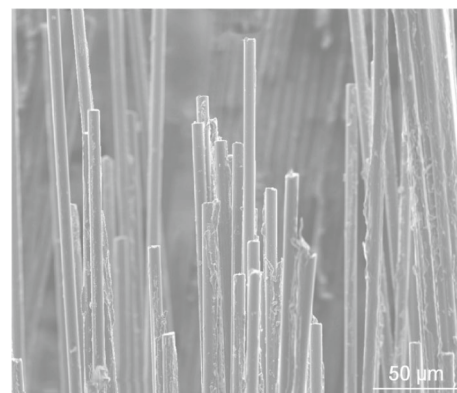
(A) $R = 0.1$, $\sigma_{max} = 1000$ MPa, $N_f = 170$



(B) $R = 0.1$, $\sigma_{max} = 1000$ MPa, $N_f = 170$

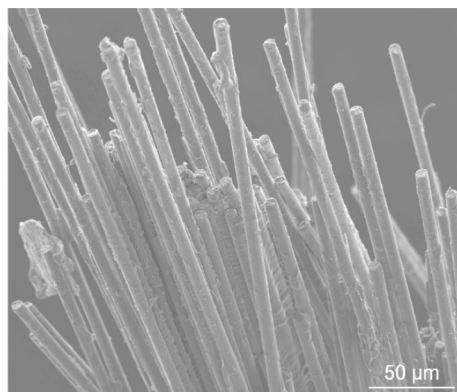


(C) $R = 0.1$, $\sigma_{max} = 350$ MPa, $N_f = 1280322$

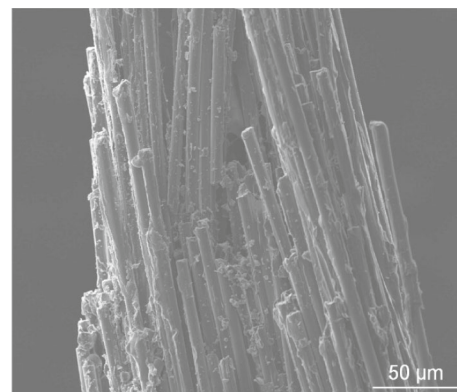


(D) $R = 0.9$, $\sigma_{max} = 850$ MPa, $N_f = 1174220$

FIGURE 6 Images of 24K3P fracture parts fractured during the fatigue tests (R : stress ratio; σ_{max} : maximum stress; and N_f : number of cycles to failure).



(A) $R = 0.1$, $\sigma_{max} = 1000$ MPa, $N_f = 1046$



(B) $R = 0.9$, $\sigma_{max} = 1800$ MPa, $N_f = 2034035$

and glass fiber in the hybrid material. σ_{CF_CFRP} and σ_{GF_GFRP} are the fiber-dominant strength of CFRP and GFRP calculated as follows:

$$\sigma_{CF_CFRP} = \frac{\sigma_{CFRP}}{VF_{CF_CFRP}} \quad (6a)$$

$$\sigma_{GF_GFRP} = \frac{\sigma_{GFRP}}{VF_{GF_GFRP}} \quad (6b)$$

The fiber-dominant strength was introduced based on the assumption that the fatigue strength of FRP is solely due to the fibers in the FRP. A detailed explanation of the fiber-dominant strength can be found in Appendix B. σ_{CFRP} and σ_{GFRP} are the strength of CFRP and GFRP. VF_{CF_CFRP} and VF_{GF_GFRP} represent the volume fraction of carbon fibers in CFRP and glass fibers in GFRP, respectively.

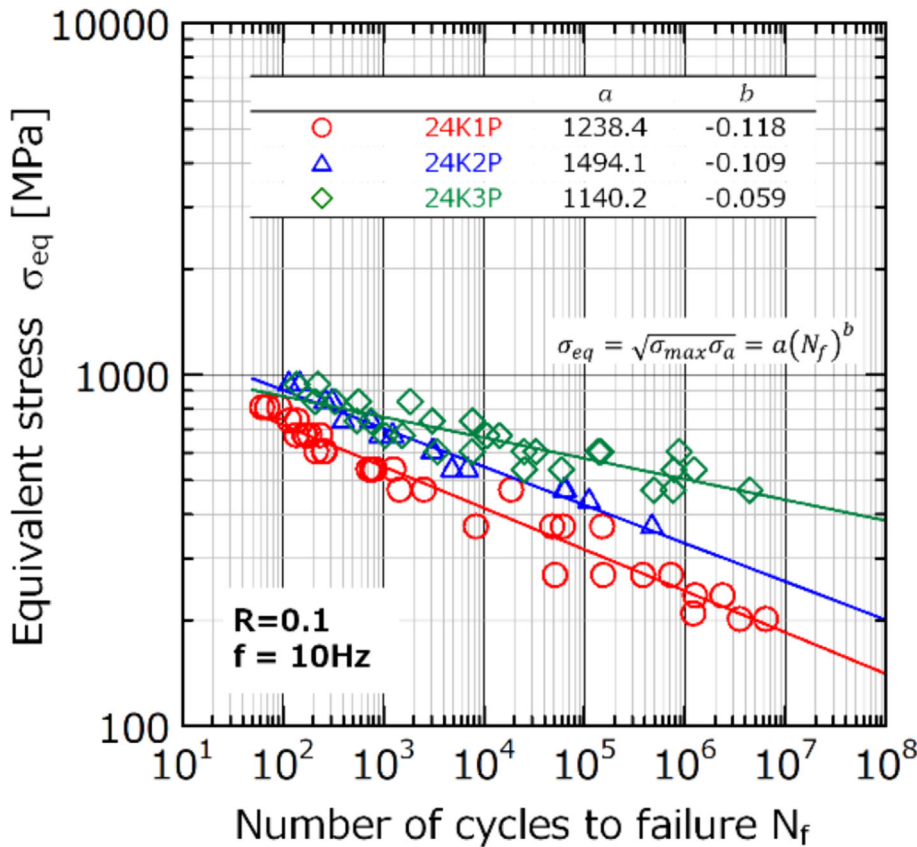


FIGURE 7 Fatigue test results under $R = 0.1$. [Colour figure can be viewed at [wileyonlinelibrary.com](https://onlinelibrary.wiley.com/doi/10.1111/ffe.14332)]

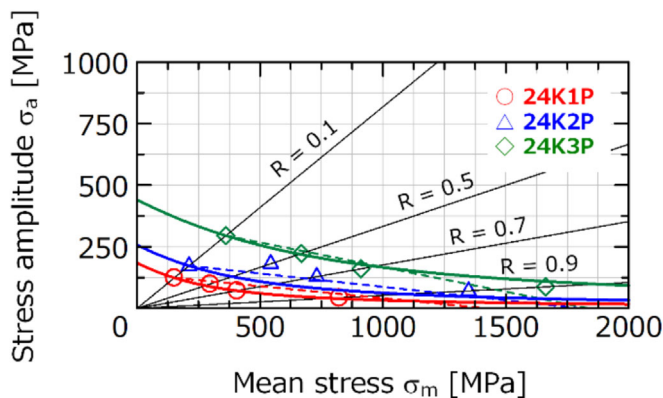


FIGURE 8 Constant life diagram for 10^7 loading cycles (line: Equation 4; dashed line: connected fatigue strength at 10^7 cycles under $R = 0.1$ and tensile strength). [Colour figure can be viewed at [wileyonlinelibrary.com](https://onlinelibrary.wiley.com/doi/10.1111/ffe.14332)]

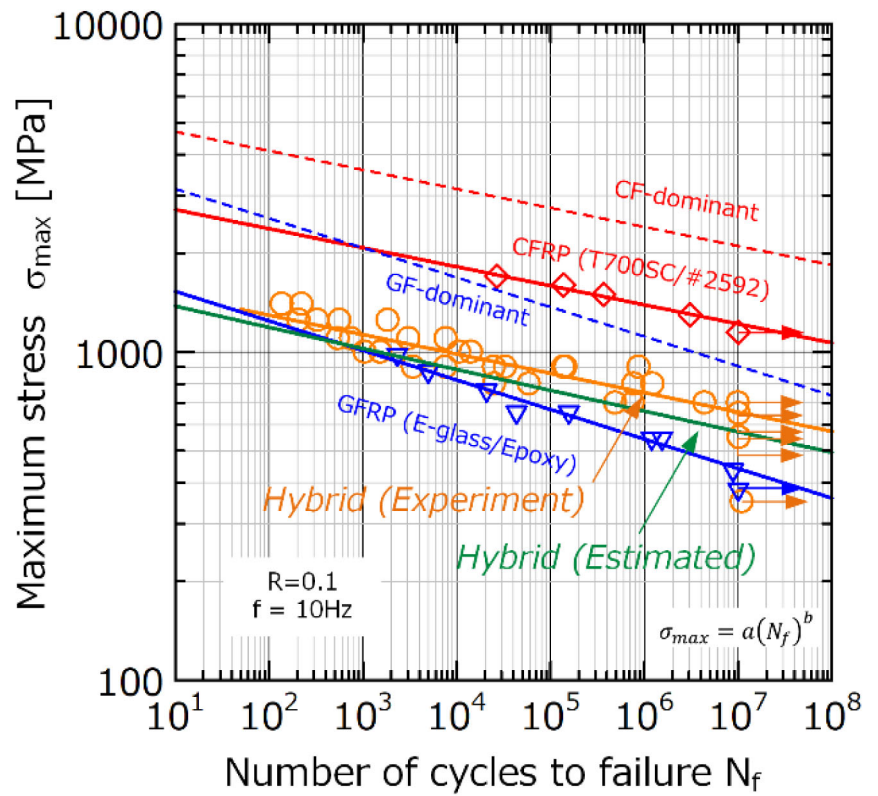
That case was validated under specific stress ratio condition; that is, the fatigue behavior of the hybrid rod under $R = 0.1$ was predicted using CFRP and GFRP fatigue test data under the same stress ratio. In this study, fatigue test data were obtained under several stress ratio conditions, and the fatigue strength prediction method was validated, including the effect of mean stress.

Here, the fatigue strength of 24K3P (VF_{CF} : 46.2%, VF_{GF} : 23.2%, $\theta = 35.2^\circ$) at 10^7 cycles is estimated. The

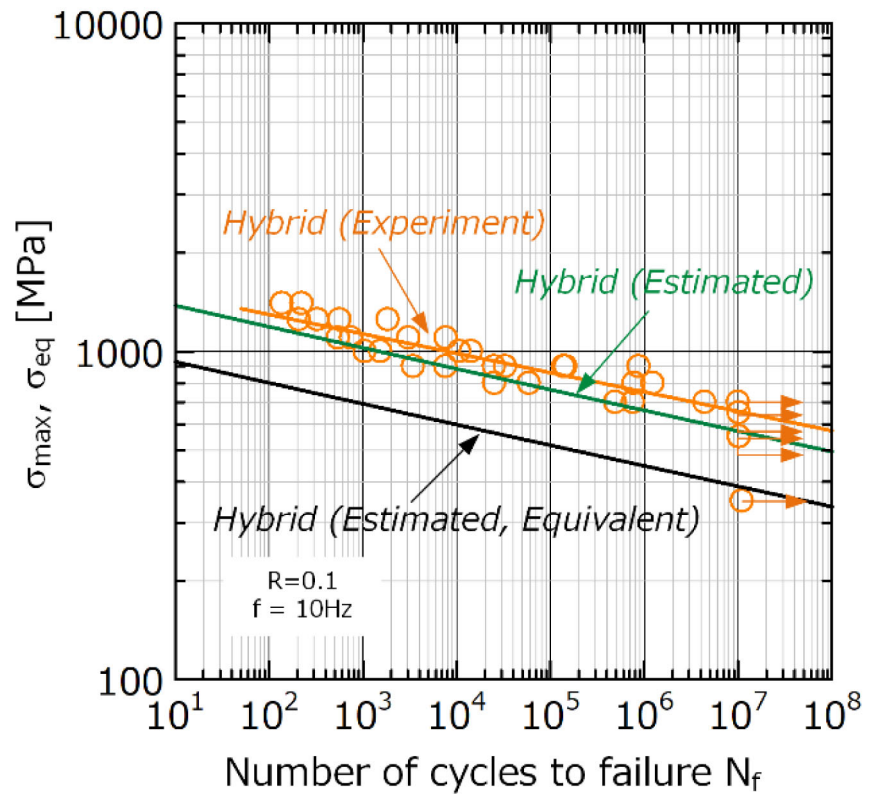
fatigue test data obtained by unidirectional CFRP (T700SC/#2592, VF_{CF_CFRP} : 57.9%, Toray Industries, Inc.) and GFRP (E-glass/180°C-cured-type epoxy, VF_{GF_GFRP} : 48.7%, Arisawa Mfg. Co., Ltd) under $R = 0.1$ are summarized in Figure 9A. The estimated line of the hybrid rod from Equations (5) and (6), which is indicated by a green line in the figure, illustrates the test data. In addition, the equivalent stress amplitude was calculated by Equation (3); as shown in Figure 9B, the fatigue strength at 10^7 cycles was calculated by using Equation (4), and the relation between mean stress and stress amplitude was estimated. The line obtained from this process and the fatigue strength at 10^7 cycles from the test data are shown in Figure 10. This figure clearly shows that the estimated line could describe the test results very well.

The fatigue strength of the hybrid rod, including the influence of mean stress, can be predicted based on the constituents of the rod with a weighted average efficiency and equivalent stress amplitude. This is probably due to the simple core-in-sheath structure of the hybrid rod; that is, the CFRP and GFRP parts exist inside and outside the rod separately, while cross-interactions are expected to be relatively smaller. This method is expected to support the prediction of fatigue strength properties and design of hybrid materials.

FIGURE 9 Prediction of the fatigue behavior 24K3P hybrid rods. [Colour figure can be viewed at wileyonlinelibrary.com]



(A) Maximum stress



(B) Equivalent stress amplitude

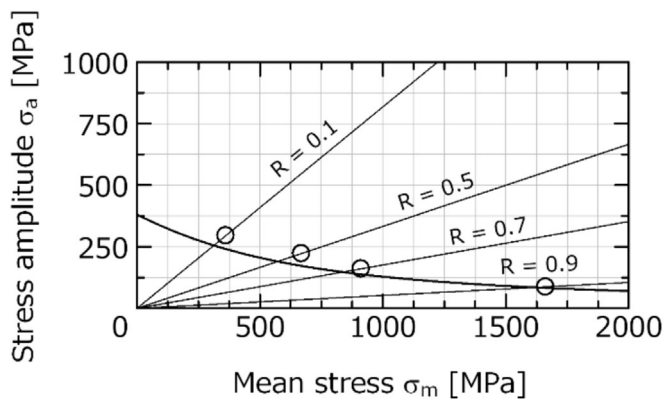


FIGURE 10 Prediction of fatigue strength at 10^7 cycles under different mean stress conditions (24K3P).

5 | CONCLUSIONS

The effect of mean stress on the fatigue properties of carbon/glass hybrid thermoplastic rods with different volume fraction of fibers was investigated, and fatigue strength at different stress ratio conditions was predicted using one fatigue data set or fatigue test data of pure CFRP and GFRP. The major conclusions of the present study can be summarized as follows.

- The difference in stress dependency of the fatigue life was more clearly observed under small stress ratio conditions. The hybrid rod with a higher volume fraction of void demonstrated a steep slope of the $S-N$ curve. This indicated that voids in the hybrid rod strongly affected fatigue properties under smaller minimum stress conditions in cyclic loading.
- The equivalent stress amplitude was introduced to consider a mean stress correction. All data points with different stress ratios almost collapse into a single line, particular at around 10^7 cycles.
- Under higher mean stress conditions, fibers were held in a tensioned state, and the effect of waviness became smaller, consequently changing the load distribution and stress dependency of the fatigue life.
- Fatigue strength under different mean stress conditions can be estimated with one $S-N$ curve of the fatigue test, and the introduction of equivalent stress amplitude is an industrially useful method to predict fatigue behavior when working with limited experimental data sets.
- The fatigue strength of hybrid rods, including the influence of mean stress, can be predicted based on their constituents by using a weighted average efficiency and equivalent stress amplitude.

AUTHOR CONTRIBUTIONS

HO designed and conducted the experiments, analyzed the data, and wrote the manuscript. KN acquired funding and edited the manuscript.

ACKNOWLEDGMENTS

This research was supported by the Ministry of Education, Culture, Sports, Science and Technology (MEXT) and the Japan Science and Technology Agency (JST) through the Center of Innovation Program “Construction of next-generation infrastructure using innovative materials”—Realization of a safe and secure society that can coexist with the Earth for centuries.

CONFLICT OF INTEREST STATEMENT

The authors declare that they have no conflict of interest.

DATA AVAILABILITY STATEMENT

The data that support the findings of this study are available from the corresponding author upon reasonable request.

ORCID

Hiroyuki Oguma  <https://orcid.org/0000-0003-1104-7317>
 Kimiyoshi Naito  <https://orcid.org/0000-0002-3334-4876>

REFERENCES

1. Sparks C, Zivanovic I, Luyckx J, Hudson W. Carbon fiber composite tendons for deepwater tension leg platforms. In: *Offshore Technology Conference*; 2003:OTC 15164.
2. Meier U. Carbon fiber reinforced polymer cables: why? why not? what if? *Arab J Sci Eng*. 2012;37(2):399-411.
3. Chandra Das S, Nizam MEH. Applications of fiber reinforced polymer composites (FRP) in civil engineering. *Int J of Adv Struct and Geotech Eng*. 2014;3:299-309.
4. Gilbert RI, Mickleborough NC. *Design of Prestressed Concrete*. Spon Press; 1990.
5. Nawy EG. *Prestressed Concrete: A Fundamental Approach, Fifth Edition Upgrade: ACI, AASHTO, IBC 2009 Codes Version*. Prentice Hall; 2009.
6. Wang L, Zhang J, Xu J, Han Q. Anchorage systems of CFRP cables in cable structures—a review. *Construct Build Mater*. 2018;160:82-99.
7. Zuo P, Srinivasan DV, Vassilopoulos AP. Review of hybrid composites fatigue. *Compos Struct*. 2021;274:114358.
8. Vassilopoulos AP. The history of fiber-reinforced polymer composite laminate fatigue. *Int J Fatigue*. 2020;134:105512.
9. Rathore DK, Prusty RK, Mohanty SC, Singh BP, Ray BC. In-situ elevated temperature flexural and creep response of interply glass/carbon hybrid FRP composites. *Mech Mater*. 2017; 105:99-111.
10. Naito K, Oguma H. Tensile properties of novel carbon/glass hybrid thermoplastic composite rods. *Compos Struct*. 2017;161: 23-31.
11. Swolfs Y, Gorbatiikh L, Verpoest I. Fibre hybridisation in polymer composites: a review. *Compos a*. 2014;67:181-200.

12. KOMATSU. *Matere Fabric Laboratory* [fa-bo] <https://www.komatsumatere.co.jp/cabkoma/en/fabo.html> [accessed 1 Nov. 2023]
13. Naito K, Oguma H. Tensile properties of novel carbon/glass hybrid thermoplastic composite rods under static and fatigue loading. *Matéria (Rio J)*. 2017;22(2):e-11843.
14. Naito K, Nagai C. Effects of temperature and water absorption on the interfacial mechanical properties of carbon/glass-reinforced thermoplastic epoxy hybrid composite rods. *Compos Struct*. 2022;282:115103.
15. Naito K, Oguma H, Nagai C. Temperature-dependent tensile properties of hybrid carbon/glass thermoplastic composite rods. *Polym Compos*. 2020;41(10):3985-3995.
16. Tanks J, Naito K. UV durability assessment of a thermoplastic epoxy-based hybrid composite rod for structural reinforcement and retrofitting. *J Build Eng*. 2022;48:103922.
17. Oguma H, Naito K. Hybridization effects on the fatigue properties of novel core-in-sheath-type carbon/glass hybrid thermoplastic composite rods. *Fatigue Fract Eng Mater Struct*. 2022; 45(12):3514-3523.
18. Brunbauer J, Pinter G. Effect of mean stress and fiber volume content on the fatigue-induced damage mechanism in CFRP. *Int J Fatigue*. 2015;75:28-38.
19. Kawai M. A phenomenological model for off-axis fatigue behavior of unidirectional polymer matrix composites under different stress ratios. *Compos A Appl Sci Manuf*. 2004;35(7-8): 955-963.
20. El Kadi H, Ellyin F. Effect of stress ratio on the fatigue of unidirectional glass fibre/epoxy composite laminae. *Compos*. 1994; 25(10):917-924.
21. *Fixing structures of fiber reinforced plastics cables and its fabrication, strength testing methods, and strength testing specimens*. National Institute for Materials Science, KOMATSU SEIREN Co., Ltd. Japanese Patent Application No.: 2017-020217; 2017. Japanese.
22. *Attachment Structure for Fiber Reinforced Plastic Cable, Manufacturing Method for Same, Strength Test Method, and Sample for Strength Test*. KOMATSU SEIREN Co., Ltd. Application No.: WO2016JP65928A; 2017.
23. Agarwal BD, Broutman LJ. *Analysis and Performance of Fiber Composites*. Wiley; 1980.
24. Talreja R. Damage and fatigue in composites—a personal account. *Comp Sci Tech*. 2008;68(13):2585-2591.
25. Harris B, Reiter H, Adam T, Dickson RF, Fernando G. Fatigue behaviour of carbon fibre reinforced plastics. *Composite*. 1990; 21(3):232-242.
26. Vassilopoulos AP, Keller T. *Fatigue of fiber-reinforced composite*. Springer; 2011.
27. Smith KN, Watson P, Topper TH. A stress strain function for the fatigue of metals. *J Mater*. 1970;5:767-778.

How to cite this article: Oguma H, Naito K. Effects of mean stress on the fatigue properties of core-in-sheath-type carbon/glass hybrid thermoplastic composite rods: Experimental investigation and practical predictive method. *Fatigue Fract Eng Mater Struct*. 2024;47(8): 2922-2933. doi:10.1111/ffe.14332

APPENDIX A: MATERIAL CHARACTERISTICS

The materials tested involved carbon/glass hybrid thermoplastic rods. Each rod had a core-in-sheath structure consisting of carbon fiber bundle(s) covered with outer braided glass fibers. The core carbon fiber bundle is surrounded by a braid of glass fibers in a sheath-core structure and gently twisted to improve abrasion

resistance and bending strength. Three types of hybrid rods with different carbon fiber contents and carbon/glass fiber ratios were used. The physical and mechanical properties of the hybrid rods are summarized in Tables A1 and A2, respectively. The braid angle (θ) was defined as the orientation angle of the interlacing yarns with respect to the longitudinal axis of the rod (see Figure 1). The volume fraction of each constituent is listed in Table A3.

	Diameter d [mm]		Braid angle θ [°]		Density ρ_h [g/cm ³]
	Ave.	SD	Ave.	SD	
24K1P	2.30	0.03	22.3	1.6	1.759
24K2P	2.73	0.04	30.2	1.5	1.737
24K3P	3.09	0.03	35.2	1.8	1.698

TABLE A1 Physical properties of the hybrid rods.

TABLE A2 Volume fractions of the hybrid rod constituents.

	Carbon fiber VF_{CF} [%]		Glass fiber VF_{GF} [%]		Matrix VF_M [%]		Void VF_V [%]	
	Ave.	SD	Ave.	SD	Ave.	SD	Ave.	SD
24K1P	24.58	1.20	39.75	0.79	25.49	0.37	10.18	0.76
24K2P	38.34	0.68	29.63	0.41	24.54	0.32	7.49	0.60
24K3P	46.18	2.79	23.15	1.93	23.39	0.67	7.28	1.33

TABLE A3 Mechanical properties of the hybrid rods.

	Tensile modulus E_L [GPa]		Poisson's ratio ν_{LT}		Tensile strength $\sigma_{L,ult}$ [MPa]		Failure strain $\epsilon_{L,ult}$ [%]	
	Ave.	SD	Ave.	SD	Ave.	SD	Ave.	SD
24K1P	65	3	0.39	0.08	1423	55	2.18	0.07
24K2P	87	7	0.41	0.10	1804	64	2.13	0.15
24K3P	91	7	0.45	0.07	1837	54	2.08	0.14

APPENDIX B: THE CONCEPT OF FIBER-DOMINANT STRENGTH

The concept of the fiber-dominant strength is described in Figure B1. The figure shows the stress–strain relation. It is assumed that the strength of FRP is dominated by the strength of fibers in FRP and proportional to the

amount of fibers, and the contribution of the polymer matrix is considered negligible compared to that of the fibers.

For example, if a high level of CFRP strength can be achieved with a small amount of carbon fibers (low VF_{CF_CFRP}), this can be interpreted as a high level of strength with 100% carbon fibers.

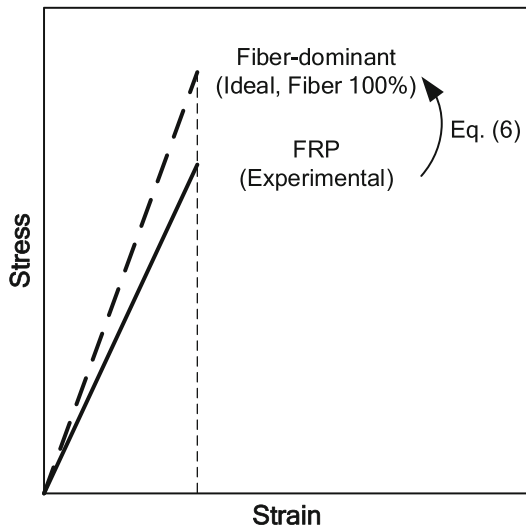


FIGURE B1 The concept of fiber-dominant strength.